Records of Natural Products

Open Access
This article is licensed under CC-BY-NC-ND 4.0

www.acgpubs.org

SHORT REPORT

Cytotoxic activities and *in silico* study of carbazole alkaloids isolated from *Murraya koenigii* against HL-60 and HeLa cancer cell lines

Ying-Xin Chew[1], Mohd Azlan Nafiah[2] and Siow-Ping Tan[1*]

[1]Department of Physical Sciences, Faculty of Applied Sciences, Tunku Abdul Rahman University of Management and Technology, 53300 Kuala Lumpur, Malaysia
[2]Department of Chemistry, Faculty of Science and Mathematics, Universiti Pendidikan Sultan Idris, 39500 Tanjong Malim, Perak, Malaysia

Abstract: Carbazole alkaloids from *Murraya koenigii* exhibit diverse structural features and promising anticancer potential. This study evaluated the cytotoxic activity and structure–activity relationship (SAR) of 24 carbazole alkaloids against HL-60 and HeLa cancer cell lines, alongside molecular docking studies against the anti-apoptotic protein Bcl-2 (PDB ID: 2W3L). The SAR analysis revealed that electron-donating and redox-active substituents, particularly formyl groups, significantly enhanced cytotoxicity, while dimerization generally reduced potency. Docking results showed binding energies ranging from −5.49 to −9.37 kcal/mol, with key interactions mainly involving Phe63, Asp70, Phe71, Met74, Val92, Glu95, Leu96, Asp99, Gly104, Phe109, Glu111 and Phe112 residues. Potent compounds such as mahanine **(15)** and murrayamine-J **(18)** exhibited both strong cytotoxicity (IC_{50} = 12.1 and 5.1 µg/mL for HL-60 and 12.8 and 7.7 µg/mL for HeLa, respectively) and favorable binding affinities (−7.66 and −7.25 kcal/mol), suggesting that Bcl-2 inhibition contributes to their activity. Conversely, murrayafolline-A **(2)** displayed notable cytotoxicity (IC_{50} = 8.5 µg/mL for HL-60 and 4.6 µg/mL for HeLa) despite only moderate predicted affinity (−5.71 kcal/mol), indicating possible alternative mechanisms of action. Similarly, bisisomahanine **(24)** showed the strongest predicted binding (−9.37 kcal/mol) with lowest ligand efficiency but negligible cytotoxicity, suggesting that the high binding affinity is attributed to its bulky size. Overall, this study provides supportive computational insights into the cytotoxic potential of carbazole alkaloids and highlights their predictive relevance for future mechanistic and pharmacokinetic studies.

Keywords: *Murraya koenigii*, carbazole alkaloids, structure-activity relationship, HL-60, HeLa, Bcl-2

Cite this article as:
Chew et al. Cytotoxic activities and *in silico* study of carbazole alkaloids isolated from *Murraya koenigii* against HL-60 and HeLa cancer cell lines. (2026). *Records of Natural Products*, 20(1):e25083616

Received: *28 August 2025*
Revised: *31 October 2025*
Accepted: *01 November 2025*
Published: *14 November 2025*

1 Plant Source

The bark and leaves of *M. koenigii* (Linn.) Spreng (TM1006) was collected from Jerantut, Pahang, Malaysia in March 2012. The voucher specimen is deposited at the herbarium of Chemistry Department, Faculty of Science and Mathematics, University Pendidikan Sultan Idris, Malaysia.

2 Previous Studies

Acute promyelocytic leukemia (e.g., HL-60 cell line) is a life-threatening hematologic malignancy (O'Connell et al., 2011). Although these treatments are clinically effective, they are associated with significant toxicities, including cardiotoxicity, hepatotoxicity, and differentiation syndrome (Iyer et al., 2023). Cervical cancer, modeled by the HeLa cell line, is another major global health burden, ranking as the fourth most common cancer in women, with more than 600,000 new cases and more than 340,000 deaths reported annually (He et al., 2024). Current treatment options include radiotherapy, targeted therapy, and immunotherapy, which, while effective, are difficult to promote due to high costs and severe side effects (Kroschinsky et al., 2017). Therefore, there is an urgent need for safer and more targeted therapeutic alternatives and natural products have gained increasing attention as sources of anticancer agents.

Among them, carbazole derivatives have gained interest because they are known to exhibit many notable biological activities, including antioxidant, antimicrobial, anti-inflammatory, antifungal and anticancer effects (Çapan et al., 2023; Hieda et al., 2014; Song et al., 2022). These compounds also reported to induce apoptosis and inhibit tumor

*Corresponding Author: Siow-Ping Tan.
Email: tansp@tarc.edu.my

Copyright © 2025. Published by ACG Publications.

cell proliferation through diverse mechanisms (Utaipan et al., 2017; Wang et al., 2016). *Murraya koenigii (M. koenigii)*, belonging to the Rutaceae family, is widely used in culinary and traditional medicine across Southeast Asia (Buathong & Duangsrisai, 2023). Our previous studies also showed that the extracts from its bark, leaves, fruits, and roots are rich in carbazole alkaloids (Tan et al., 2020, 2017; Ahmad et al., 2015; Tan et al., 2014, 2015).

Computational approach by using molecular docking offers a valuable insight into the binding interactions of carbazole alkaloids with the anti-apoptotic protein B-cell lymphoma 2 (Bcl-2), complementing experimental cytotoxicity studies. Bcl-2 plays an important role in inhibiting the permeabilization of mitochondrial outer membrane by binding to pro-apoptotic proteins which prevents the release of cytochrome-c and the subsequence activation of downstream caspases. This allow cancer cells to evade programmed cell death since bcl-2 are overexpressed in HL-60 and HeLa cells compared to the normal cells, contributing to their sustained survival and resistance to apoptotic triggers. By targeting Bcl-2, it can restore the cancer cell's apoptotic sensitivity and thereby contributing to their cytotoxicity effect (Toure et al., 2013).

In the present study, 24 carbazole alkaloids previously isolated from the bark and leaves of *M. koenigii* (Tan et al., 2015) were used to examine for their structure–activity relationship (SAR) based on the *in vitro* cytotoxic activities against HL-60 and HeLa cell lines. The *in vitro* cytotoxic activities were also performed on MRC-5 and NIH/3T3 which act as normal cell lines to evaluate the compounds' selectivity, and vincristine (VCR) will be used as the positive control. In addition, pharmacokinetic behaviors were evaluated by examining the absorption, distribution, metabolism, and excretion (ADME) properties to access the drug-likeness and identify possible liabilities. To provide mechanistic insight, molecular docking was performed against of Bcl-2 (PDB ID: 2W3L, Chain A) using AutoDock 4.2, and binding interactions were analyzed with Discovery Studio Visualizer (Toure et al., 2013). By integrating SAR analysis with docking, this study aims to elucidate structural features that modulate both cytotoxic potency and Bcl-2 binding affinity, thereby advancing the potential of *M. koenigii* carbazole alkaloids as leads for anticancer drug discovery.

3 Present Study

The isolation of various carbazole alkaloids from the bark and leaves of *M. koenigii* were reported in our previous study (Tan et al., 2015). These carbazole alkaloids can be categoried according to five classes: tricyclic carbazoles, quinone-type tricyclic carbazoles, pyrano[3,2-a]carbazoles, cyclic monoterpenoid pyrano[3,2-a]carbazoles, and biscarbazoles. In brief, the cytotoxic activities of these alkaloids were assessed using the MTT [3-(4,5-dimethylthiazol-2-yl)-2,5-diphenyltetrazolium bromide] assay against human promyelocytic leukaemia cell lines (HL-60), cervical cancer cell lines (HeLa), normal human lung fibroblasts (MRC-5), and mouse embryonic fibroblasts (NIH/3T3) cell lines *in vitro*. Briefly, cells were seeded in 96-well plates and incubated overnight at 37 °C in a humidified atmosphere with 5% CO_2 to allow attachment (for HeLa cells), followed by treatment with varying concentrations of the compounds. After 72 hours of incubation, 20 µL of MTT solution (5 mg/mL in PBS) was added to each well and incubated for 4 h at 37 °C, after which the medium was carefully removed and the purple formazan crystals formed were solubilized with 100 µL of dimethyl sulfoxide (DMSO). The absorbance was measured at 570 nm with a reference wavelength of 630 nm using a microplate reader, and cell viability was calculated relative to untreated control cells using the formula: Cell viability (%) = $(A_{sample}/A_{control}) \times 100$, where A_{sample} and $A_{control}$ is the absorbance of treated and control cells, respectively. The cytotoxic activities (the IC_{50} values) against HL-60 and HeLa cell lines were recorded. The results were then considered for SAR analysis which focused on key structural features such as electron-donating/withdrawing groups, ring system variations, side chains, and dimerization.

Molecular docking was used to predict the binding affinity of ligands towards the receptor proteins. The crystal structure of the anti-apoptotic protein Bcl-2 (PDB ID: 2W3L, Chain A) was retrieved from the Protein Data Bank (https://www.rcsb.org) (Toure et al., 2013). All crystallographic water molecules and co-crystallized ligands were removed prior to docking. Polar hydrogens were added, and Kollman charges were assigned using AutoDockTools 1.5.6 (Morris et al., 2009). Docking studies were carried out with AutoDock 4.2 (Morris et al., 2009), and the receptor and ligand files were saved in PDBQT format for subsequent docking. The chemical structures of neutral carbazole alkaloids were drawn and the energy was minimized using Chem3D. Each ligand was converted into PDBQT format using AutoDockTools for subsequent docking. The docking grid was positioned over the enzyme's active site with the centre coordinates (X, Y, Z = 41.320, 27.687, −12.684) and grid dimensions (X, Y, Z = 60, 60, 52). The docking protocol was validated by re-docking the native ligand (ABT-737) into the active site, yielding an RMSD value of 1.0040 Å (≤2.0 Å) (Supporting Information–Figure S1). This docked pose corresponded to the top-ranked conformation based on binding affinity, confirming the accuracy and consistency of the docking results. AutoGrid was performed to generate the grid file. The docking parameters were chosen to be 10 genetic algorithm runs, 150 population size and medium evaluation. The best docked conformation with the most favourable binding energy was selected for further analysis on the enzyme-ligand interactions. Docking poses were visualized and analyzed using Discovery Studio Visualizer (BIOVIA, San Diego, CA, USA, 2020). The keys protein-ligand interactions, such as hydrogen bonds, hydrophobic interaction, and electrostatic interactions, were recorded (Figure 1, Supporting Information–Figure S2). Key interacting residues were identified and compared across compounds to elucidate shared binding motifs. The pharmacokinetic properties of the carbazole alkaloids were predicted using SwissADME (Daina et al., 2017). The SMILES strings for the compounds were generated from the 2D structures using ChemDraw and were used as an input on the website.

http://doi.org/10.25135/rnp.2508.3616
Rec. Nat. Prod. 2026, 20(1):e25083616

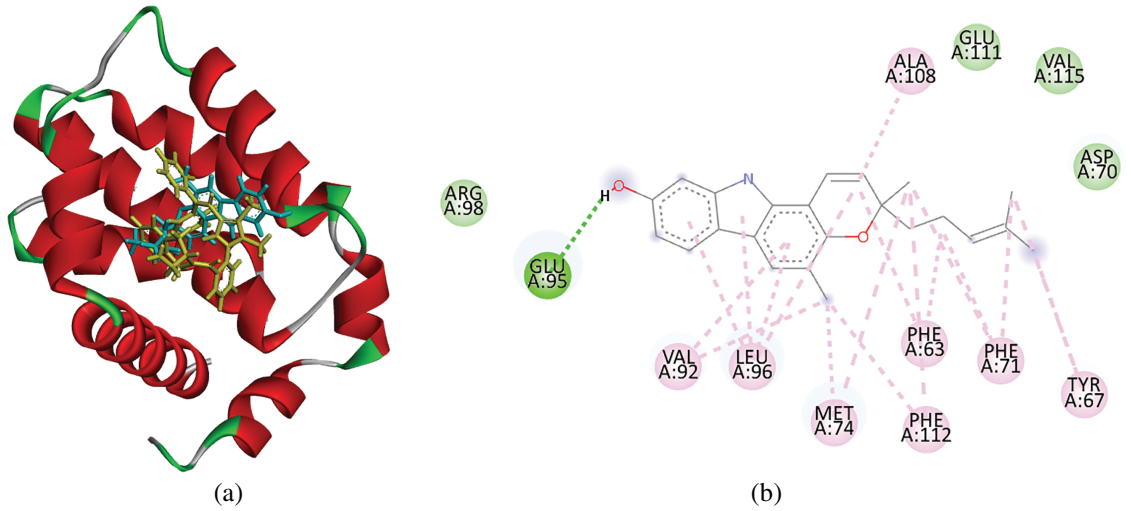

Figure 1. Docking poses of the most biologically relevant compound Mahanine (**15**) (blue) with the Bcl-2 protein (PDB ID: 2W3L), compared with the native inhibitor ABT-737 (yellow): (a) with complex pymol and (b) 2D interaction map. Different colors indicate various interaction types: Hydrogen bonds (green dashed lines), electrostatic interactions (orange dashed lines), hydrophobic interaction (other colours)

Consensus LogP, topological polar surface area (TPSA) and Lipinski rule of five violations were obtained.

For tricyclic carbazoles **(1–8)**, *in vitro* cytotoxicity was generally weak cytotoxicity, except for murrayafolline-A **(2)**, which exhibited IC_{50} values of 8.5 µg/mL (HL-60) and 4.6 µg/mL (HeLa). (Table 1). This may be attributed to the presence of the two electro-donating groups (ortho-OCH_3 and and para-CH_3), suggesting that moderate electron donating can favorably influence cytotoxic effects. However, the docking results revealed only moderate binding affinity (−5.71 kcal/mol) with mainly hydrophobic interactions with Phe63, Tyr67, Phe71, Leu96 and Ala108 (Table 2, Supporting Information–Figure S2). This suggested that murrayafolline-A **(2)** may exert cytotoxicity via mechanisms other than direct Bcl-2 inhibition, such as DNA intercalation, oxidative stress induction or interaction with other protein targets (Rebekky & Chakraborty, 2007), although further experimental validation is required. Mahanimbilol **(6)**, Euchrestine-B **(7)** and mukoenine-B **(8)** showed a relatively higher docking scores (−6.47, −6.58 and −6.08 kcal/mol, respectively) but weak cytotoxicity potency, together with a lower ligand efficiencies, implying that the observed docking affinities may be achieved by molecular size rather than efficient per atom interactions (Tables 1 and 2) (Kenny, 2019). For quinone-type tricyclic carbazoles **(9–10)**, the quinone moiety likely contribute to cytotoxicity through redox-active nature, such as ROS generation or covalent modification. Murrayaquinone-A **(9)** and murrayaquinone-B **(10)** showed IC_{50} values of 16.0 and 39.0 µg/mL (HL-60) and 36.7 and 6.6 µg/mL (HeLa), respectively, with docking energies of −5.63 and −6.17 kcal/mol. Murrayaquinone-A **(9)** displays higher ligand efficiency compared to murrayaquinone-B **(10)**, suggesting a more favourable interaction per atom (Table 2).

Among pyrano[3,2-a]carbazoles **(11–18)**, several compounds demonstrated stronger cytotoxic activities, which were correlated with more favourable docking scores. Among them, mahanine **(15)** and murrayamine-J **(18)** showed potent cytotoxicity with IC_{50} value of 12.1 and 5.1 µg/mL for HL-60 and 12.8 and 7.7 µg/mL for HeLa, respectively, and showed strong predicted binding scores of −7.66 and −7.25 kcal/mol (Tables 1 and 2). Their predicted interactions, such as hydrogen bond (Glu95 and Asp99) and multiple hydrophobic contacts (Phe63, Tyr67, Phe71, Met74, Val92, Leu96, Ala108 and Phe112) (Figure 1, Supporting Information–Figure S2), suggested that Bcl-2 inhibition contributes significantly to their bioactivity. Similarly, isomahanine **(16)** displayed relatively favourable docking scores (−7.11 kcal/mol) with an H-bond to Asp99, but its lower cellular potency and reduced ligand efficiency suggest that steric bulk and poor efficiency per atom may limit its biological effect (Table 2). Mono-substituted derivates containing either electron-donating or electron-withdrawing group at C-3 including girinimbine **(11)**, murrayacine **(13)** and mahanimbine **(14)** are generally moderate to weak in cytotoxic activity, congruent with their less favourable docking energies (−6.60 to −7.57 kcal/mol) (Tables 1 and 2).

For cyclic monoterpenoid pyrano[3,2-a]carbazoles **(19–21)**, cytotoxicity was moderate while for murrayakoeninol **(20)** and bicyclomahanimbine **(21)** show relatively favorable docking (−7.78 and −7.49 kcal/mol). These ligands interact with several pocket residues (Phe63, Asp70, Phe71, Met74, Val92, Glu95, Leu96, Asp99, Gly104, Phe109, Glu111 and Phe112), primarily via hydrophobic contacts (Table 2, Supporting Information–Figure S2). Their ligand efficiencies are comparable, and the result indicates that the binding have a moderate interaction with the ligand. This discrepancy between their binding affinity and moderate cytotoxicity may be attributed to entropic penalties due to structural flexibility, or limited bioavailability in cellular environments (Lipinski et al., 2001; Dong et al., 2021).

Table 1. IC_{50} values after treatment 72 h against HL-60, HeLa, MRC-5 and NIH/3T3 cell lines

Compounds	Structures	R^1	R^2	R^3	R^4	R^5	HL-60	HeLa	MRC-5	NIH/3T3
									IC_{50} (μg/mL)	
Tricyclic carbazole										
Murrayanine **(1)**		OCH_3	H	CHO	H	H	40.4	>60	>100	>60
Murrayafolline-A **(2)**		OCH_3	H	CH_3	H	H	8.5	4.6	>100	>60
Koenoline **(3)**		OCH_3	H	CH_2OH	H	H	41.1	47.8	>100	>60
3-formylcarbazole **(4)**	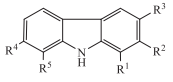	H	H	CHO	H	H	44.2	28.7	>100	>60
2-hydroxy-3-methylcarbazole **(5)**		H	OH	CH_3	H	H	35.7	39.1	>100	>60
Mahanimbilol **(6)**		Geranyl	OH	CH_3	H	H	>60	39.1	>100	>60
Euchrestine-B **(7)**		H	OH	CH_3	Geranyl	Geranyl	41.4	19.8	>100	>60
Mukoenine-B **(8)**		Geranyl	OH	CHO	H	H	52.1	>60	>100	>60
Carbazole-1,4-quinone carbazole alkaloids										
Murrayaquinone-A **(9)**	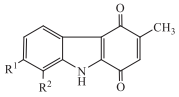	H	H				16.0	36.7	>100	>60
Murrayaquinone-B **(10)**		OCH_3	Geranyl				39.0	6.6	>100	>60
Pyrano[3,2-a]carbazole alkaloids										
Girinimbine **(11)**		CH_3	H	H	H	CH_3	34.8	12.2	>100	>60
Koenimbine **(12)**		CH_3	OCH_3	H	H	CH_3	15.8	40.6	>100	>60
Murrayacine **(13)**		CHO	H	H	H	CH_3	47.4	45.0	>100	>60
Mahanimbine **(14)**	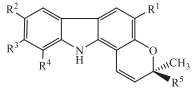	CH_3	H	H	H	Prenyl	38.2	21.4	>100	>60
Mahanine **(15)**		CH_3	H	OH	H	Prenyl	12.1	12.8	>100	>60
Isomahanine **(16)**		H	CH_3	OH	H	Prenyl	>60	27.7	>100	>60
Murrayamine-B **(17)**		CH_3	H	H	OCH_3	Prenyl	46.8	36.9	>100	>60
Murrayamine-J **(18)**		H	CHO	H	H	Prenyl	5.1	7.7	>100	>60
Cyclic monoterpenoid pyrano[3,2-1]carbazole alkaloids										
Murrayazolinol **(19)**	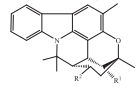	H	OH				42.2	46.0	>100	>60
Murrayakoeninol **(20)**		OH	H				46.6	18.1	>100	>60
Bicyclomahanimbine **(21)**	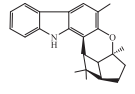						31.7	19.6	>100	>60
Biscarbazole alkaloids										
Bismurrayafoline-E **(22)**	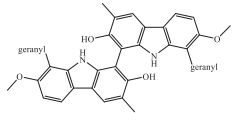						42.9	>60	>100	>60
Bispyrayafoline **(23)**	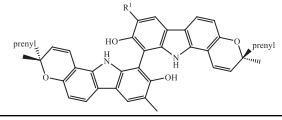	H					>60	45.7	>100	>60
Bisisomahanine **(24)**		CH_3					>60	>60	>100	>60

Table 2. The molecular docking results of carbazole alkaloids **(1–24)**

Compounds	Binding energy (ΔG, kcal/mol)	Ligand efficiency	Amino acid involved and its interaction		
			Hydrophobic interaction	Aromatic stacking	Hydrogen bond
Murrayanine **(1)**	−5.63	0.331	Tyr67, Asp70, Met74, Val92, Leu96, Phe112	Phe63, Phe71, Ala108	Phe71
Murrayafoline-A **(2)**	−5.71	0.357	Tyr67, Asp70, Phe71, Met74, Val92, Leu96, Phe112	Phe63, Ala108	–
Koenoline **(3)**	−5.64	0.332	Tyr67, Asp70, Met74, Val92, Leu96, Phe109, Phe112, Ala108	–	Phe71
3-formylcarbazole **(4)**	−5.56	0.371	Asp70, Phe71, Met74, Val92, Leu96, Ala108, Phe109, Phe112	Phe63	Tyr67, Phe71
2-hydroxy-3methylcarbazole **(5)**	−5.49	0.366	Tyr67, Phe71, Met74, Val92, Ala108, Phe109, Phe112	Phe63	Asp70
Mahanimbilol **(6)**	−6.47	0.259	Phe63, Asp70, Met74, Val92, Leu96, Arg105, Ala108, Phe109, Glu111, Phe112	Phe71	Tyr67
Euchrestine-B **(7)**	−6.58	0.244	Tyr67, Asp70, Phe71, Met74, Val92, Val93, Glu95, Leu96, Arg105, Ala108, Phe109, Glu111, Phe112	Phe63	–
Mukoenine-B **(8)**	−6.08	0.234	Phe63, Asp70, Phe71, Met74, Glu95, Ala108, Phe109, Glu111, Phe112, Val115	Tyr67	Val92, Leu96
Murrayaquinone-A **(9)**	−5.63	0.352	Tyr67, Asp70, Phe71, Met74, Leu96, Ala108, Phe112	Phe63	–
Murrayaquinone-B **(10)**	−6.17	0.268	Phe63, Phe71, Met74, Val92, Leu95, Arg105, Ala108, Phe109, Glu111, Phe112, Val115	Tyr67	Asp70
Girinimbine **(11)**	−6.66	0.333	Tyr67, Asp70, Met74, Leu96, Arg105, Ala108, Phe112	Phe63, Phe71	–
Koenimbine **(12)**	−6.65	0.302	Tyr67, Asp70, Phe71, Met74, Leu96, Arg105, Ala108, Phe112	Phe63	Asn102
Murrayacine **(13)**	−6.60	0.314	Phe63, Tyr67, Asp70, Phe71, Met74, Leu96, Arg105, Ala108, Phe112	–	–
Mahanimbine **(14)**	−7.57	0.303	Phe63, Tyr67, Asp70, Phe71, Met74, Val92, Glu95, Leu96, Arg98, Asp99, Arg105, Ala108, Phe109, Glu111, Phe112	–	–
Mahanine **(15)**	−7.66	0.294	Phe63, Tyr67, Asp70, Phe71, Met74, Val92, Leu96, Arg98, Ala108, Glu111, Phe112, Val115	–	–
Isomahanine **(16)**	−7.11	0.273	Phe63, Tyr67, Asp70, Phe71, Met74, Val92, Leu96, Arg98, Arg105, Ala108, Phe112	–	Asp99
Murrayamine-B **(17)**	−7.65	0.283	Phe63, Tyr67, Asp70, Phe71, Met74, Val92, Glu95, Leu96, Arg105, Ala108, Glu111, Phe112, Val115	–	–
Murrayamine-J **(18)**	−7.25	0.279	Phe63, Tyr67, Phe71, Met74, Val92, Glu95, Leu96, Phe97, Arg98, Arg105, Ala108, Phe112	–	Asp99
Murrayazolinol **(19)**	−7.58	0.292	Phe63, Asp70, Phe71, Met74, Val92, Leu96, Ala108, Phe112	Tyr67	–
Murrayakoeninol **(20)**	−7.78	0.299	Phe63, Asp70, Phe71, Met74, Leu96, Phe109, Glu111, Phe112	Tyr67	Ala108
Bicyclomahanimbine **(21)**	−7.49	0.300	Phe63, Phe71, Met74, Val92, Glu95, Leu96, Asp99, Gly104, Arg105, Ala108, Phe112	–	–
Bismurrayafoline-E **(22)**	−6.99	0.129	Phe63, Asp70, Phe71, Met74, Val92, Glu95, Leu96, Arg98, Gly104, Arg105, Ala108, Phe112	–	Tyr67
Bispyrayafoline **(23)**	−9.24	0.185	Phe63, Tyr67, Asp70, Phe71, Met74, Val92, Glu95, Leu96, Arg98, Arg105, Gly104, Ala108, Phe112	–	Asp99
Bisisomahanine **(24)**	−9.37	0.177	Phe63, Tyr67, Phe71, Met74, Val92, Leu96, Arg98, Asp99, Asn102, Gly104, Arg105, Ala108, Phe109, Phe112	–	*Electrostatic aromatic:* Glu95
ABT-737 (native Bcl-2 inhibitor)	−9.05	0.162	Phe63, Phe71, Val92, Glu95, Leu96, Gly104, Arg105, Ala108, Phe112	Tyr67, Met74	Asp70

Table 3. Drug-likeness parameters of carbazole alkaloids are based on Lipinski's rule of five

Compound	Mol. formula	TPSA (Å^2)	Mol. weight	Log P	H-bond acceptors	H-bond donors	Lipiski's rule of 5 violation
Murrayanine **(1)**	$C_{14}H_{11}NO_2$	42.09	225.24	2.69	3	1	0
Murrayafoline-A **(2)**	$C_{14}H_{13}NO$	25.02	211.26	3.31	2	1	0
Koenoline **(3)**	$C_{14}H_{13}NO_2$	45.25	227.26	2.49	3	2	0
3-formylcarbazole **(4)**	$C_{13}H_9NO$	32.86	195.22	2.68	2	1	0
2-hydroxy-3methylcarbazole **(5)**	$C_{13}H_{11}NO$	36.02	197.23	2.93	2	2	0
Mahanimbilol **(6)**	$C_{23}H_{27}NO$	36.02	333.47	5.82	2	2	1
Euchrestine-B **(7)**	$C_{24}H_{29}NO_2$	45.25	363.49	5.75	3	2	1
Mukoenine-B **(8)**	$C_{23}H_{27}NO_2$	56.25	349.47	5.01	3	3	1
Murrayaquinone-A **(9)**	$C_{13}H_9NO_2$	49.93	211.22	2.15	3	1	0
Murrayaquinone-B **(10)**	$C_{19}H_{19}NO_3$	59.16	309.36	3.65	4	1	0
Girinimbine **(11)**	$C_{18}H_{17}NO$	25.02	263.33	4.17	2	1	0
Koenimbine **(12)**	$C_{19}H_{19}NO_2$	34.25	293.36	4.15	3	1	0
Murrayacine **(13)**	$C_{18}H_{15}NO_2$	42.09	277.32	3.56	3	1	0
Mahanimbine **(14)**	$C_{23}H_{25}NO$	25.02	331.45	5.62	2	1	1
Mahanine **(15)**	$C_{23}H_{25}NO_2$	45.25	347.45	5.20	3	2	1
Isomahanine **(16)**	$C_{23}H_{27}NO_2$	45.25	337.46	5.00	3	2	1
Murrayamine-B **(17)**	$C_{24}H_{27}NO_2$	34.25	361.48	5.61	3	1	1
Murrayamine-J **(18)**	$C_{23}H_{25}NO_2$	34.25	347.45	5.29	3	1	1
Murrayazolinol **(19)**	$C_{23}H_{25}NO_2$	34.39	347.45	4.14	3	1	0
Murrayakoeninol **(20)**	$C_{23}H_{25}NO_2$	34.39	347.45	4.19	3	1	0
Bicyclomahanimbine **(21)**	$C_{23}H_{25}NO$	25.02	331.45	5.21	2	1	1
Bismurrayafoline-E **(22)**	$C_{48}H_{56}N_2O_4$	90.50	724.97	5.21	6	4	2
Bispyrayafoline **(23)**	$C_{46}H_{48}N_2O_2$	50.04	660.89	10.39	6	4	2
Bisisomahanine **(24)**	$C_{47}H_{50}N_2O_4$	90.50	706.91	10.33	6	4	2

Biscarbazoles **(22–24)** generally exhibited weak activity, consistent with previous reports that dimerization of monomeric scaffolds can reduce cytotoxic potency (Paquin, Reyes-Moreno & Bérubé, 2021; Bednarczyk-Cwynar & Günther, 2017). However, bisisomahanine **(24)** presented the most favorable docking score (−9.37 kcal/mol), mediated by multiple hydrophobic interaction and electrostatic interaction (including a π–anion contact with Glu95) (**Supporting Information–Figure S2**). However, its low ligand efficiency and lack of corresponding *in vitro* activity suggest that the high docking score may be largely size-driven and that other factors (desolvation, entropy, permeability) limit cellular efficacy.

Carbazole alkaloids from *M. koenigii* display diverse cytotoxic activities depending on their structural features. The SAR study revealed that electron-donating and redox-active groups enhance anticancer potential, while pyrano and dimeric structures reduce efficacy. Moreover, these findings also suggest that while Bcl-2 inhibition may contribute to the activity of certain carbazole alkaloids, other mechanisms are also likely involved, and future work should explore multi-target effects and pharmacokinetic properties to fully understand their anticancer potential.

Table 3 summarizes the drug-likeness parameters of 24 carbazole alkaloids evaluated using computational tools. Most compounds meet Lipinski's rule of five, indicating good oral bioavailability potential. Specifically, most compounds have molecular weights below 500 Da, log P values below 5, ≤10 hydrogen bond acceptors, and ≤5 hydrogen bond donors. No rule violations were observed for compounds **1–20**, indicating good drug-likeness. Compounds with one undesirable behavior (**6–8**, **14–18**, **21**) primarily exhibited higher log P values, indicating enhanced lipophilicity. The molecular weights and log P values of dimeric carbazoles (**22–24**) were outside the limits, indicating low oral bioavailability. Overall, the results suggest that most monomeric carbazole alkaloids meet standard drug-likeness criteria and are promising candidates for further optimization, while dimeric analogs may require structural modifications to enhance pharmacokinetic properties.

In conclusion, this study demonstrates that carbazole alkaloids exhibit potent cytotoxicity against HL-60 and HeLa cells, but minimal toxicity against normal cells. Molecular docking analysis further confirmed that these compounds may interact with the anti-apoptotic protein Bcl-2, suggesting that their cytotoxicity may be mechanistically related to apoptosis. However, as Bcl-2 is only one of several potential targets involved in apoptosis regulation, this explanation remains speculative. Therefore, future studies will include mechanistic analyses to confirm the role of Bcl-2 and other related pathways, as well as advanced computational studies such as molecular dynamics simulations, quantitative structure-activity relationship binding free energy analysis to reinforce the current computer modeling results.

http://doi.org/10.25135/rnp.2508.3616
Rec. Nat. Prod. 2026, 20(1):e25083616

Acknowledgement

Authors acknowledge the financial support by TAR UMT Publication Incentive under vote head FOAS/PS/86000-4923. We also thank Universiti Pendidikan Sultan Idris for providing research facilities.

Funding Statement

Authors acknowledge the financial support by TAR UMT Publication Incentive under vote head FOAS/PS/86000-4923.

Author Contributions

Chew Y.X. conceived and designed the study, performed the experiments, and drafted the manuscript; Nafiah M.A. analyzed the data and contributed to data interpretation and manuscript revision; Tan S.P. analyzed the data, supervised the project, provided resources, and reviewed and edited the final manuscript.

Availability of Data and Materials

The authors declare that the data supporting the findings of this study are available within the paper and its Supplementary Information files. Should any raw data files be needed in another format they are available from the corresponding author upon reasonable request. Source data are provided with this paper.

Conflict of Interest

The authors declare they have no conflict of interest.

Supporting Information

Supporting information accompanies this paper on http://www.acgpubs.org/journal/records-of-natural-products.

ORCID

Ying-Xin Chew: 0009-0006-0003-3613
Mohd Azlan Nafiah: 0000-0002-8221-9430
Siow-Ping Tan: 0000-0002-5861-6962

References

Ahmad, K., Tan, S. P., Hazni, H. & Nafiah, M. A. (2015). Cyclic Monoterpenoid pyranocarbazole alkaloids from the bark of *Murraya koenigii* (L.) Spreng. *Jurnal Teknologi*, *77*(2), 73–77. DOI: 10.11113/jt.v77.5990.

Bednarczyk-Cwynar, B. & Günther, A. (2017). Advances in chemistry and pharmacology of triterpenoid synthetic dimers. *Current Medicinal Chemistry*, *24*(20), 2205–2240. DOI: 10.2174/0929867324666170202151625.

Buathong, R. & Duangsrisai, S. (2023). Plant ingredients in Thai food: a well-rounded diet for natural bioactive associated with medicinal properties. *Peer J*, *11*(6), e14568. DOI: 10.7717/peerj.14568.

Çapan, İ., Hawash, M., Jaradat, N., Sert, Y., Selvi, R. & Koca, İ. (2023). Design, synthesis, molecular docking and biological evaluation of new carbazole derivatives as anticancer, and antioxidant agents. *BMC Chemistry*, *17*(1), 60. DOI: 10.1186/s13065-023-00961-y.

Daina, A., Michielin, O. & Zoete, V. (2017). SwissADME: a free web tool to evaluate pharmacokinetics, drug-likeness and medicinal chemistry friendliness of small molecules. *Scientific Reports*, *7*(1), 42717. DOI: 10.1038/srep42717.

Dong, L., Qu, X., Zhao, Y. & Wang, B. (2021). Prediction of binding free energy of protein-ligand complexes with a hybrid molecular mechanics/generalized born surface area and machine learning method. *ACS Omega*, *6*(48), 32938–32947. DOI: 10.1021/acsomega.1c04996.

He, L., Qian, H., Yang, C., Shi, N., Chen, C., Zhang, P. & Hou, Y. (2024). CD133+/ABCC5+ cervical cancer cells exhibit cancer stem cell properties. *Heliyon*, *10*(17), e37066. DOI: 10.1016/j.heliyon.2024.e37066.

Hieda, Y., Anraku, M., Choshi, T., Tomida, H., Fujioka, H., Hatae, N., Hori, O., Hirose, J. & Hibino, S. (2014). Antioxidant effects of the highly substituted carbazole alkaloids and their related carbazoles. *Bioorganic & Medicinal Chemistry Letters*, *24*(15), 3530–3533. DOI: 10.1016/j.bmcl.2014.05.050.

Iyer, G., Elias, L., Stanchina, M. & Watts, J. (2023). The treatment of acute promyelocytic leukemia in 2023: paradigm, advances, and future directions. *Frontiers in Oncology*, *12*, 1062524. DOI: 10.3389/fonc.2022.1062524.

Kenny, P. W. (2019). The nature of ligand efficiency. *Journal of Cheminformatics*, *4*, 74–114.

Kroschinsky, F., Stölzel, F., von Bonin, S., Beutel, G., Kochanek, M., Kiehl, M., Schellongowski, P., Intensive Care in Hematological and Oncological Patients (iCHOP) Collaborative Group. (2017). New drugs, new toxicities: severe side effects of modern targeted and immunotherapy of cancer and their management. *Critical Care*, *21*(1), 89. DOI: 10.1186/s13054-017-1678-1.

Lipinski, C. A., Lombardo, F., Dominy, B. W. & Feeney, P. J. (2001). Experimental and computational approaches to estimate solubility and permeability in drug discovery and development settings. *Advanced Drug Delivery Reviews*, *46*(1–3), 3–26. DOI: 10.1016/s0169-409x(96)00423-1.

Morris, G. M., Huey, R., Lindstrom, W., Sanner, M. F., Belew, R. K., Goodsell, D. S. & Olson, A. J. (2009). AutoDock4 and AutoDockTools4: automated docking with selective receptor flexibility. *Journal of Computational Chemistry*, *30*(16), 2785–2791. DOI: 10.1002/jcc.21256.

O'Connell, P. A., Madureira, P. A., Berman, J. N., Liwski, R. S. & Waisman, D. M. (2011). Regulation of S100A10 by the PML-RAR-α oncoprotein. *Blood*, *117*(15), 4095–4105. DOI: 10.1182/blood-2010-07-298851.

Paquin, A., Reyes-Moreno, C. & Bérubé, G. (2021). Recent advances in the use of the dimerization strategy as a means to increase the biological potential of natural or synthetic molecules. *Molecules*, *26*(8), 2340. DOI: 10.3390/molecules26082340.

Rebekky, A., Chakraborty, D. P. (2007). Molecular modes of action of cytotoxic alkaloids: from DNA intercalation, spindle poisoning, topoisomerase inhibition to apoptosis and multiple drug

resistance. *Bioorganic & Medicinal Chemistry*, *15*, 436–454. DOI: 10.1016/s1099-4831(07)64001-2.

Song, F., Liu, D., Huo, X. & Qiu, D. (2022). The anticancer activity of carbazole alkaloids. *Archiv der Pharmazie*, *355*(1), 2100277. DOI: 10.1002/ardp.202100277.

Tan, S. P., Ali, A. M., Nafiah, M. A., Amna, U., Ramli, S. A. & Ahmad, K. (2017). Terpenes and phenolic compounds from *Murraya koengii*. *Chemistry of Natural Compounds*, *53*(5), 980–981. DOI: 10.1007/s10600-017-2177-y.

Tan, S. P., Ali, A. M., Nafiah, M. A., Awang, K. & Ahmad, K. (2015). Isolation and cytotoxic investigation of new carbazole alkaloids from *Murraya koenigii* (Linn.) Spreng. *Tetrahedron*, *71*(23), 3946–3953. DOI: 10.1016/j.tet.2015.04.037.

Tan, S. P., Lim, S. M., Wong, M. K., Lim, C. Y. & Nafiah, M. A. (2020). Chemical constituents from *Murraya koenigii* (L.) Spreng berries. *Chemistry of Natural Compounds*, *56*(5), 962–963. DOI: 10.1007/s10600-020-03202-z.

Tan, S. P., Nafiah, M. A. & Ahmad, K. (2014). C23-carbazole alkaloids from Malayan *Murraya koenigii* (L.) Spreng. *Journal of Chemical and Pharmaceutical Research*, *6*(4), 1093–1098.

Toure, B. B., Miller-Moslin, K., Yusuff, N., Perez, L., Dore, M., Joud, C., Michael, W., DiPietro, L., van der Plas, S., McEwan, M., Lenoir, F., Hoe, M., Karki, R., Springer, C., Sullivan, J., Levine, K., Fiorilla, C., Xie, X., Kulathila, R., Herlihy, K., et al. (2013). The role of the acidity of N-heteroaryl sulfonamides as inhibitors of bcl-2 family protein-protein interactions. *ACS Medicinal Chemistry Letters*, *4*(2), 186–190. DOI: 10.1021/ml300321d.

Utaipan, T., Athipornchai, A., Suksamrarn, A., Jirachotikoon, C., Yuan, X., Lertcanawanichakul, M. & Chunglok, W. (2017). Carbazole alkaloids from *Murraya koenigii* trigger apoptosis and autophagic flux inhibition in human oral squamous cell carcinoma cells. *Journal of Natural Medicines*, *71*(1), 158–169. DOI: 10.1007/s11418-016-1045-6.

Wang, W., Sun, X., Sun., D., Li, S., Yu, Y., Yang, T., Yao, J., Chen, Z. & Duan, L. (2016). Carbazole aminoalcohols induce antiproliferation and apoptosis of human tumor cells by inhibiting Topoisomerase I. *ChemMedChem*, *11*(24), 2675–2681. DOI: 10.1002/cmdc.201600391.